Regulation of inorganic carbon acquisition in a red tide alga (*Skeletonema costatum*): the importance of phosphorus availability

Guang Gao[a,b,c], Jianrong Xia[a*], Jinlan Yu[a], Jiale Fan[b], Xiaopeng Zeng[a]

[a]School of Environmental Science and Engineering, Guangzhou University, Guangzhou, 510006, China

[b]Jiangsu Key Laboratory of Marine Bioresources and Environment, Huaihai Institute of Technology, Lianyungang, 222005, China

[c]State Key Laboratory of Marine Environmental Science, Xiamen University, Xiamen 361005, China

[*]Corresponding author, Email: jrxia@gzhu.edu.cn; Phone: +86 (0)20 39366941; Fax: +86 (0)20 39366949

Abstract:

Skeletonema costatum is a common bloom-forming diatom and encounters eutrophication and severe carbon dioxide (CO_2) limitation during red tides. However, little is known regarding the role of phosphorus (P) in modulating inorganic carbon acquisition in *S. costatum*, particularly under CO_2 limitation conditions. We cultured *S. costatum* under five phosphate levels (0.05, 0.25, 1, 4, 10 μmol L^{-1}) and then treated it with two CO_2 conditions (2.8 and 12.6 μmol L^{-1}) for two hours. The lower CO_2 reduced net photosynthetic rate at lower phosphate levels (< 4 μmol L^{-1}) but did not affect it at higher phosphate levels (4 and 10 μmol L^{-1}). In contrast, the lower CO_2 induced higher dark respiration rate at lower phosphate levels (0.05 and 0.25 μmol L^{-1}) and did not affect it at higher phosphate levels (> 1 μmol L^{-1}). The lower CO_2 did not change relative electron transport rate (rETR) at lower phosphate levels (0.05 and 0.25 μmol L^{-1}) and increased it at higher phosphate levels (> 1 μmol L^{-1}). Photosynthetic CO_2 affinity ($1/K_{0.5}$) increased with phosphate levels. The lower CO_2 did not affect photosynthetic CO_2 affinity at 0.05 μmol L^{-1} phosphate but enhanced it at the other phosphate levels. Activity of extracellular carbonic anhydrase was dramatically induced by the lower CO_2 at phosphate replete conditions (> 0.25 μmol L^{-1}) and the same pattern also occurred for redox activity of plasma membrane. Direct bicarbonate (HCO_3^-) use was induced when phosphate concentration was more than 1 μmol L^{-1}. These findings indicate P enrichment could enhance inorganic carbon acquisition and thus maintain the photosynthesis rate in *S. costatum* grown under CO_2 limiting conditions via increasing activity of extracellular carbonic anhydrase and facilitating direct HCO_3^- use. This study sheds light on how bloom-forming algae cope with carbon limitation during the development of red tides.

Keywords: carbonic anhydrase; CO_2 concentrating mechanisms; pH compensation point; photosynthesis; redox activity; respiration

1. Introduction

Diatoms are unicellular photosynthetic microalgae that can be found worldwide in freshwater and oceans. Marine diatoms account for 75% of the primary productivity for coastal and other nutrient-rich zones and approximately 20% of global primary production (Field *et al.*, 1998; Falkowski, 2012), hence playing a vital role in the marine biological carbon pump as well as the biogeochemical cycling of important nutrients, such as nitrogen and silicon (Nelson *et al.*, 1995; Moore *et al.*, 2013; Young & Morel, 2015). Diatoms usually dominate the phytoplankton communities and form large-scale blooms in nutrient–rich zones and upwelling regions (Bruland *et al.*, 2001; Anderson *et al.*, 2008; Barton *et al.*, 2016). Nutrient enrichment is considered as a key factor that triggers algal blooms albeit the occurrence of diatom blooms may be modulated by other environmental factors, such as temperature, light intensity, salinity, and so forth (Smetacek & Zingone, 2013; Jeong *et al.*, 2015). When inorganic nitrogen and phosphorus are replete, diatoms can out-compete chrysophytes, raphidophytes and dinoflagellates (Berg *et al.*, 1997; Jeong *et al.*, 2015; Barton *et al.*, 2016) and dominate algal blooms due to their quicker nutrient uptake and growth rate.

In normal natural seawater (pH 8.1, salinity 35), HCO_3^- is the majority (~90%) of total dissolved inorganic carbon (DIC, 2.0–2.2 mM). CO_2 (1%, 10–15 μM), which is the only direct carbon source that can be assimilated by all photosynthetic organisms, only accounts for 1% of total dissolved inorganic carbon. Diatoms' ribulose-1,5-bisphosphate carboxylase/oxygenase (Rubisco), catalyzing the primary chemical reaction by which CO_2 is transformed into organic carbon, has a relatively low affinity for CO_2 and is commonly less than half saturated under current CO_2 levels in seawater (Hopkinson & Morel, 2011),

suggesting that CO_2 is limiting for marine diatoms' carbon fixation. To cope with the CO_2 limitation in seawater and maintain a high carbon fixation rate under the low CO_2 conditions, diatoms have evolved various inorganic carbon acquisition pathways and CO_2 concentrating mechanisms (CCMs), for instance, active transport of HCO_3^-, the passive influx of CO_2, multiple carbonic anhydrase (including both common (α, β, γ, found in all algae) and unusual (δ, ζ, found only in diatoms) families that carries out the fast interconversion of CO_2 and HCO_3^-), assumed C4-type pathway (using phosphoenolpyruvate to capture more CO_2 in the periplastidal compartment), to increase the concentration at the location of Rubisco and thus the carbon fixation. (Hopkinson & Morel, 2011; Hopkinson *et al.*, 2016). *Skeletonema costatum* is a worldwide diatom species that can be found from equatorial to polar waters. It usually dominates large-scale algal blooms in eutrophic seawaters (Wang, 2002; Li *et al.*, 2011). When blooms occur, seawater pH increases and CO_2 decreases because the dissolution rate of CO_2 from the atmosphere cannot catch up with its removal rate caused by intensive photosynthesis of algae. For instance, pH level in the surface waters of the eutrophic Mariager Fjord, Denmark, could be up to 9.75 during algal blooms (Hansen, 2002). Consequently, *S. costatum* experiences very severe CO_2 limitation when blooms occur. To deal with it, *S. costatum* has developed multiple CCMs (Nimer *et al.*, 1998; Rost *et al.*, 2003). However, contrasting findings were reported. Nimer *et al.* (1998) documented that extracellular carbonic anhydrase activity in *S. costatum* was only induced when CO_2 concentration was less than 5 μmol L^{-1} while Rost *et al.* (2003) reported that activity of extracellular carbonic anhydrase could be detected even when CO_2 concentration was 27 μmol L^{-1}. Chen and Gao (2004) showed that ~~in~~ *S. costatum* had little capacity in direct HCO_3^- utilization. On the other hand,

Rost *et al.* (2003) demonstrated that this species could take up CO_2 and HCO_3^- simultaneously.

Phosphorus (P) is an indispensable element for all living organisms, serving as an integral component of lipids, nucleic acids, adenosine-triphosphate (ATP) and a diverse range of other metabolites. Levels of bioavailable phosphorus are very low in many ocean environments and phosphorus enrichment can commonly increase algal growth and marine primary productivity in the worldwide oceans (Davies & Sleep, 1989; Müller & Mitrovic, 2015; Lin *et al.*, 2016). Due to the essential role of phosphorus, extensive studies have been conducted to investigate the effect of phosphorus on photosynthetic performances (Geider *et al.*, 1998; Liu *et al.*, 2012; Beamud *et al.*, 2016), growth (Jiang *et al.*, 2016; Reed *et al.*, 2016; Mccall *et al.*, 2017), phosphorus acquisition, utilization and storage (Lin *et al.*, 2016; Gao et al., 2018a). Some studies show the essential role of phosphorus in regulating inorganic carbon acquisition in green algae (Beardall *et al.*, 2005; Hu & Zhou, 2010). In terms of *S. costatum*, studies regarding the inorganic carbon acquisition in *S. costatum* focus on its response to variation of CO_2 availability. The role of phosphorus in *S. costatum*'s CCMs remains unknown. Based on the connection between phosphorus and carbon metabolism in diatoms (Brembu *et al.*, 2017), we hypothesize that phosphorus enrichment could enhance inorganic carbon utilization and hence maintain high rates of photosynthesis and growth in *S. costatum* under CO_2 limitation conditions. In the present study, we aimed to test this hypothesis by investigating the variation of CCMs (including active transport of HCO_3^- and carbonic anhydrase activity) and photosynthetic rate under five levels of phosphate and two levels of CO_2 conditions. We also measured redox activity of plasma membrane as it is deemed to be critical to activate carbonic

anhydrase (Nimer *et al.*, 1998). Our study ~~would~~ provides helpful insights into how bloom-forming diatoms overcome CO_2 limitation to maintain a quick growth rate during red tides.

2. Materials and Methods

2.1. Culture conditions

Skeletonema costatum (Grev.) Cleve from Jinan University, China, was cultured in f/2 artificial seawater with five phosphate levels (0.05, 0.25, 1, 4, 10 μmol L^{-1}) by adding different amounts of $NaH_2PO_4 \cdot 2H_2O$. The cultures were carried out semi-continuously at 20°C for seven days. The light irradiance was set as 200 μmol photons m^{-2} s^{-1}, with a light and dark period of 12: 12. The cultures were aerated with ambient air (0.3 L min^{-1}) to maintain the pH around 8.2. The cells during exponential phase were collected and rinsed twice with DIC-free seawater that was made according to Xu *et al.* (2017). Afterwards, cells were resuspended in fresh media with two levels of pH (8.20 and 8.70, respectively corresponding to ambient CO_2 (12.6 μmol L^{-1}~~, AC~~) and low CO_2 (2.8 μmol L^{-1}~~, LC~~) under corresponding phosphate levels for two hours before the following measurements, with a cell density of 1.0×10^6 mL^{-1}. The concentrations of DIC were 2109 ± 36 and 1802 ± 38 μmol (kg seawater)$^{-1}$, respectively. Cell density was determined by direct counting with an improved Neubauer haemocytometer (XB-K-25, Qiu Jing, Shanghai, China). This transfer aimed to investigate the effects of phosphate on DIC acquisition under a CO_2 limitation condition. The pH of 8.70 was chosen considering that it is commonly used as a CO_2 limitation condition (Nimer *et al.*, 1998; Chen & Gao, 2004) and also occurs during algal blooms (Hansen, 2002). Two hours should be enough to activate CCMs in *S. costatum* (Nimer *et al.*, 1998). The cell

density did not vary during the two hours of pH treatment. All experiments were conducted in triplicates.

2.2. Manipulation of seawater carbonate system

The two levels of pH (8.20 and 8.70) were obtained by aerating the ambient air and pure nitrogen (99.999%) ~~till~~until the target value, and were then maintained with a buffer of 50 mM tris (hydroxymethyl) aminomethane-HCl. The cultures were open to the ambient atmosphere and the rise of culture pH was due to algal photosynthesis below 0.02 unit~~e~~s (corresponding to the ~~rise~~ decrease of CO_2 less than 0.7 and 0.2 μmol L^{-1} for pH 8.20 and 8.70 treatments, respectively) during the two hours of pH treatment. CO_2 level in seawater was calculated via CO2SYS (Pierrot *et al.*, 2006) based on measured pH and TAlk, using the equilibrium constants of K1 and K2 for carbonic acid dissociation (Roy *et al.*, 1993) and the KSO_4^- dissociation constant from Dickson (1990).

~~2.3.~~ The pH_{NBS} was measured by a pH meter (pH 700, Eutech Instruments, Singapore) that was equipped with an Orion® 8102BN Ross combination electrode (Thermo Electron Co., USA) and calibrated with standard National Bureau of Standards (NBS) buffers (pH = 4.01, 7.00, and 10.01 at 25.0 °C; Thermo Fisher Scientific Inc., USA). Total alkalinity (TAlk) was determined at 25.0 °C by Gran acidimetric titration on a 25-ml sample with a TAlk analyzer (AS-ALK1, Apollo SciTech, USA), using the precision pH meter and an Orion® 8102BN Ross electrode for detection. To ensure the accuracy of TAlk, the TAlk analyser was regularly calibrated with certified reference materials from Andrew G. Dickson's laboratory (Scripps Institute of Oceanography, U.S.A.) at a precision of ±2 μmol kg^{-1}. ~~CO_2 level in seawater was calculated via CO2SYS (Pierrot *et al.*, 2006) based on measured pH and TAlk, using the~~

带格式的：字体：（默认）Times New Roman，小四，字体颜色：文字 1

带格式的：正文，无项目符号或编号

~~equilibrium constants of K1 and K2 for carbonic acid dissociation (Roy *et al.*, 1993) and the KSO_4^- dissociation constant from Dickson (1990).~~

2.3. Chlorophyll fluorescence measurement

Chlorophyll fluorescence was measured with a pulse modulation fluorometer (PAM-2100, Walz, Germany) to assess electron transport in photosystem II (the first protein complex in the light-dependent reactions of photosynthesis) and the possible connection between electron transport and redox activity of the plasma membrane. The measuring light and actinic light were 0.01 and 200 µmol photons m^{-2} s^{-1}, respectively. The saturating pulse was set 4,000 µmol photons m^{-2} s^{-1} (0.8 s). ~~Relative e~~Electron transport in photosystem II (~~r~~ETR, µmol e^- (mg Chl *a*)~~$^{-1}$~~ s^{-1}) ~~=~~ = 0.5 × E × Φ_{PSII} × $\bar{a}^*$ (Dimier *et al.*, 2009; Alderkamp *et al.*, 2012), where E (µmol photons m^{-2} s^{-1}) is the ambient light density, Φ_{PSII} (dimensionless) is the PSII photochemical efficiency and $\bar{a}^*$ is Chl *a*–specific absorption coefficient (m^{-2} (mg Chl *a*)$^{-1}$). Since $\bar{a}^*$ is light-dependent, we used the value of 0.0138 based on Lefebvre *et al*'s (2007) study in which the light density is very close to ours.

~~(F_M' – F_t) / F_M' × 0.5 × PFD (Gao et al., 2018), where F_M' is the maximal fluorescence levels from algae in the actinic light after application a saturating pulse, Ft is the fluorescence at an excitation level and PFD is the actinic light density.~~

2.4. Estimation of photosynthetic oxygen evolution and respiration

The net photosynthetic and respiration rates of *S. costatum* were measured using a Clark-type oxygen electrode (YSI Model 5300, USA) that was held in a circulating water bath (Cooling Circulator; Cole Parmer, Chicago, IL, USA) to keep the setting temperature (20°C). Five mL of samples were transferred to the oxygen electrode cuvette and were stirred during

带格式的：字体：倾斜

measurement. The light intensity and temperature were maintained as the same as that in the growth condition. The illumination was provided by a halogen lamp. The increase of oxygen content in seawater within five minutes was defined as net photosynthetic rate. To measure dark respiration rate, the samples were placed in darkness and the decrease of oxygen content within ten minutes was defined as dark respiration rate given the slower oxygen variation rate for dark respiration. Net photosynthetic rate and dark respiration rate were presented as μmol O_2 $(10^9$ cells$)^{-1}$ h^{-1}.

To obtain the curve of net photosynthetic rate versus DIC, seven levels of DIC (0, 0.1, 0.2, 0.5, 1, 2, and 4 mM) were made by adding different amounts of $NaHCO_3$ to the Tris buffered DIC-free seawater (pH 8.20). The algal samples were washed twice with DIC-free seawater before transferring to the various DIC solutions. Photosynthetic rates at different DIC levels were measured under saturating irradiance of 400 μmol photons m^{-2} s^{-1} and growth temperature. The algal samples were allowed to equilibrate for 2–3 min at each DIC level during which period a linear change in oxygen concentration was obtained and recorded. The parameter, photosynthetic half saturation constant ($K_{0.5}$, i.e., the DIC concentration required to give half of DIC-saturated maximum rate of photosynthetic O_2 evolution), was calculated from the Michaelis-Menten kinetics equation (Caemmerer and Farquhar 1981): $V = V_{max} \times [S] / (K_{0.5} + [S])$, where V is the real-time photosynthetic rate, V_{max} is maximum photosynthetic rate and [S] is the DIC concentration. The value of $1/ K_{0.5}$ represents photosynthetic DIC affinity. $K_{0.5}$ for CO_2 was calculated via CO2SYS (Pierrot *et al.*, 2006) based on pH and TA, using the equilibrium constants of K1 and K2 for carbonic acid dissociation (Roy *et al.*, 1993) and the KSO_4^- dissociation constant from Dickson (1990).

179 *2.5. Measurement of photosynthetic pigment*

180 To determine the photosynthetic pigment (Chl *a*) content, 50 mL of culture were filtered
181 on a Whatman GF⁄F filter, extracted in 5 mL of 90% acetone for 12 h at 4^{o}C, and centrifuged
182 (3, 000 *g*, 5 min). The optical density of the supernatant was scanned from 200 to 700 nm
183 with a UV-VIS spectrophotometer (Shimadzu UV-1800, Kyoto, Japan). The concentration of
184 Chl *a* was calculated based on the optical density at 630 and 664 nm: Chl $a = 11.47 \times OD_{664} -$
185 $0.40 \times OD_{630}$ (Gao et al., 2018b), and was normalized to pg cells^{-1}.

186 *2.6. Measurement of extracellular carbonic anhydrase activity*

187 Carbonic anhydrase activity was assessed using the electrometric method (Gao *et al.*,
188 2009). Cells were harvested by centrifugation at 4, 000 *g* for five minutes at 20^{o}C, washed
189 once and resuspended in 8 mL Na-barbital buffer (20 mM, pH 8.2). Five mL CO_2-saturated
190 icy distilled water was injected into the cell suspension, and the time required for a pH
191 decrease from 8.2 to 7.2 at 4^{o}C was recorded. Extracellular carbonic anhydrase (CA_{ext})
192 activity was measured using intact cells. CA activity (E.U.) was calculated using the
193 following formula: $E.U. = 10 \times (T_0 / T - 1)$, where T_0 and T represent the time required for the
194 pH change in the absence or presence of the cells, respectively.

195 *2.7. Measurement of redox activity in the plasma membrane*

196 The redox activity of plasma membrane was assayed by monitoring the change in
197 $K_3Fe(CN)_6$ concentration that accompanied reduction of the ferricyanide to ferrocyanide. The
198 ferricyanide [$K_3Fe(CN)_6$] cannot penetrate intact cells and has been used as an external
199 electron acceptor (Nimer *et al.*, 1998; Gao *et al.*, 2018b). Stock solutions of $K_3Fe(CN)_6$ were
200 freshly prepared before use. Five mL of samples were taken after two hours of incubation

with 500 μmol $K_3Fe(CN)_6$ and centrifuged at 4000 g for 10 min (20°C). The concentration of $K_3Fe(CN)_6$ in the supernatant was measured spectrophotometrically at 420 nm (Shimadzu UV-1800, Kyoto, Japan). The decrease of $K_3Fe(CN)_6$ during the two hours of incubation was used to assess the rate of extracellular ferricyanide reduction that was presented as μmol $(10^6 \text{ cells})^{-1} h^{-1}$ (Nimer et al., 1998).

2.8. Cell-driving pH drift experiment

To obtain the pH compensation point, the cells were transferred to sealed glass vials containing fresh medium (pH 8.2) with corresponding phosphate levels. The cell concentration for all treatments was 5.0×10^5 mL^{-1}. The pH drift of the suspension was monitored at 20°C and 200 μmol photons m^{-2} s^{-1} light level. The pH compensation point was obtained when there was no ~~a~~ further increase in pH.

2.9. Statistical analysis

Results were expressed as means of replicates ± standard deviation and data were analyzed using the software SPSS v.21. The data from each treatment conformed to a normal distribution (Shapiro-Wilk, $P > 0.05$) and the variances could be considered equal (Levene's test, $P > 0.05$). Two-way ANOVAs were conducted to assess the effects of CO_2 and phosphate on net photosynthetic rate, dark respiration rate, ratio of net photosynthetic rate to dark respiration rate, rETR, Chl *a*, $K_{0.5}$, CA_{ext}, reduction rate of ferricyanide, and pH compensation point. Least Significant Difference (LSD) was conducted for *post hoc* investigation. Repeated measures ANOVAs were conducted to analyze the effects of DIC on net photosynthetic rate and the effect of incubation time on media pH in a closed system. Bonferroni was conducted for *post hoc* investigation as it is the best reliable *post hoc* test for repeated measures ANOVA

(Ennos, 2007). The threshold value for determining statistical significance was $P < 0.05$.

3. Results

3.1. Effects of CO_2 and phosphate on photosynthetic and respiratory performances

The net photosynthetic rate and dark respiration rate in *S. costatum* grown at various CO_2 and phosphate concentrations were first investigated (Fig. 1). CO_2 interacted with phosphate on net photosynthetic rate, with each factor having a main effect (Table 1 & Fig. 1a). *Post hoc* LSD comparison ($P = 0.05$) showed that 2.8 µmol CO_2 ~~LC~~ reduced net photosynthetic rate when the phosphate levels was below 4 µmol L^{-1} but did not affect it at the higher phosphate levels. Under ~~AC~~the condition of 12.6 µmol CO_2, net photosynthetic rate increased with phosphate level and reached the plateau (100.51 ± 9.59 µmol O_2 (10^9 cells)$^{-1}$ h^{-1}) at 1 µmol L^{-1} phosphate. Under the condition of 2.8 µmol CO_2~~LC~~, net photosynthetic rate also increased with phosphate level but did not hit the peak (101.46 ± 9.19 µmol O_2 (10^9 cells)$^{-1}$ h^{-1}) until 4 µmol L^{-1} phosphate. In terms of dark respiration rate (Fig. 1b), phosphate had a main effect on it and it interacted with CO_2 (Table 1). Specifically, 2.8 µmol CO_2~~LC~~ increased dark respiration rate at 0.05 and 0.25 µmol L^{-1} phosphate levels, but did not affect it when phosphate level was above 1 µmol L^{-1} (LSD, $P < 0.05$). Regardless of CO_2 level, respiration rate increased with phosphate availability and stopped at 1 µmol L^{-1}.

The ratio of respiration to photosynthesis ranged from 0.23 to 0.40 (Fig. ~~2~~1c). Both CO_2 and phosphate had a main effect, and they interacted on the ratio of respiration to photosynthesis (Table 1). The level of 2.8 µmol CO_2~~LC~~ increased the ratio when phosphate was lower than 4 µmol L^{-1} but did not affect it when phosphate levels were 4 or 10 µmol L^{-1}.

Both CO_2 and phosphate affected ~~r~~ETR and they also showed an interactive effect (Fig. ~~3~~

2 & Table 2). For instance, *post hoc* LSD comparison showed that 2.8 μmol CO_2LC did not affect rETR at lower phosphate levels (0.05 and 0.25 μmol L^{-1}) but increased it at higher phosphate levels (1–10 μmol L^{-1}). Regardless of CO_2 treatment, rETR increased with phosphate level (0.05–4 μmol L^{-1}) but the highest phosphate concentration did not result in a further increase in rETR (LSD, $P > 0.05$).

The content of Chl *a* was measured to investigate the effects of CO_2 and phosphate on photosynthetic pigment in *S. costatum* (Fig. 43). Both CO_2 and phosphate affected the synthesis of Chl *a* and they had an interactive effect (Table 2). *Post hoc* LSD comparison (P = 0.05) showed that 2.8 μmol CO_2LC did not affect Chl *a* at 0.05 or 0.25 μmol L^{-1} phosphate but stimulated Chl *a* synthesis at higher phosphate levels (1–10 μmol L^{-1}). Irrespective of CO_2 treatment, Chl *a* content increased with phosphate level and reached the plateau (0.19 ± 0.01 pg $cell^{-1}$ for 12.6 μmol CO_2AC and 0.23 ± 0.01 pg $cell^{-1}$ for 2.8 μmol CO_2LC) at 4 μmol L^{-1} phosphate.

To assess the effects of CO_2 and phosphate on photosynthetic CO_2 affinity in *S. costatum*, the net photosynthetic rates of cells exposure to seven levels of DIC were measured (Fig. 54). After curve fitting, the values of $K_{0.5}$ for CO_2 were calculated (Fig. 65). CO_2 and phosphate interplayed on $K_{0.5}$ and each had a main effect (Table 2). The level of 2.8 μmol CO_2LC did not affect $K_{0.5}$ at the lowest phosphate level but reduced it at the other phosphate levels. Under ACthe condition of 12.6 μmol CO_2, higher phosphate levels (0.25–4 μmol L^{-1}) reduced $K_{0.5}$ and the highest phosphate level led to a further decrease to 2.59 ± 0.29 μmol kg^{-1} seawater compared to the value of 4.00 ± 0.30 μmol kg^{-1} seawater at 0.05 μmol L^{-1} phosphate. The pattern with phosphate under LCat 2.8 μmol CO_2 was the same as 12.6 μmol $CO_2$the AC.

带格式的：字体：加粗

3.3. The effects of CO_2 and phosphate on inorganic carbon acquisition

To investigate the potential mechanisms that cells overcame CO_2 limitation during algal blooms, the activity of CA_{ext}, a CCM related enzyme, was estimated under various CO_2 and phosphate conditions (Fig. ~~7a~~6a). Both CO_2 and phosphate had a main effect and they interacted on CA_{ext} activity (Table 3). *Post hoc* LSD comparison (P = 0.05) showed that 2.8 µmol CO_2~~LC~~ induced more CA_{ext} activity under all phosphate conditions except for 0.05 µmol L^{-1} levels, compared to 12.6 µmol CO_2~~AC~~. Under ~~AC~~the condition of 12.6 µmol CO_2, CA_{ext} activity increased (0.04–0.10 EU (10^6 cells)$^{-1}$) with phosphate level and stopped increasing at 1 µmol L^{-1} phosphate. Under the condition of 2.8 µmol CO_2~~LC~~, CA_{ext} activity also increased (0.04–0.35 EU (10^6 cells)$^{-1}$) with phosphate level but reached the peak at 4 µmol L^{-1} phosphate. The redox activity of plasma membrane was also assessed to investigate the factors that modulate CA_{ext} activity (Fig. ~~7b~~6b). The pattern of redox activity of plasma membrane under various CO_2 and phosphate conditions was the same as that of CA_{ext} activity. That is, CO_2 and phosphate had an interactive effect on redox activity of plasma membrane, each having a main effect (Table 3).

To test cells' tolerance to high pH and obtain pH compensation points in *S. costatum* grown under various CO_2 and phosphate levels, changes of media pH in a closed system were monitored (Fig. ~~8~~7). The media pH under all phosphate conditions increased with incubation time (Table 4). Specifically speaking, there was a steep increase in pH during the first three hours, afterwards the increase became slower and it reached a plateau in six hours (Bonferroni, P < 0.05). Phosphate had an interactive effect with incubation time (Table 4). For instance, there was no significant difference in media pH among phosphate levels during first two

hours of incubation but then divergence occurred and they stopped at different points. Two-way ANOVA analysis showed that CO_2 treatment did not affect pH compensation point but phosphate had a main effect (Table 3-). Under each CO_2 treatment, pH compensation point increased with phosphate level, with lowest of 9.03 ± 0.03 at 0.05 µmol L^{-1} and highest of 9.36 ± 0.04 at 10 µmol L^{-1} phosphate.

4. Discussion

4.1. Photosynthetic performances under various CO_2 and phosphate conditions

The lower CO_2 availability reduced the net photosynthetic rate of *S. costatum* grown at the lower phosphate levels in the present study. However, Nimer *et al.* (1998) demonstrated that the increase in pH (8.3−9.5) did not reduce photosynthetic CO_2 fixation of *S. costatum* and Chen and Gao (2004) reported that a higher pH (8.7) even stimulated the photosynthetic rate of *S. costatum* compared to the control (pH 8.2). The divergence between our and the previous studies may be due to different nutrient supply. Both Nimer *et al.* (1998) and Chen and Gao (2004) used f/2 media to grow algae. The phosphate concentration in f/2 media is ~36 µmol L^{-1}, which is replete for physiological activities in *S. costatum*. *Skeletonema costatum* grown at higher phosphate levels (4 and 10 µmol L^{-1}) also showed similar photosynthetic rates for the lower and higher CO_2 treatments. Our finding combined with the previous studies indicates phosphorus plays an important role in dealing with low CO_2 availability for photosynthesis in *S. costatum*.

Different from net photosynthetic rate, 2.8 µmol CO_2 ~~LC~~ did not affect rETR at lower phosphate levels (0.05 and 0.25 µmol L^{-1}) and stimulated it at higher phosphate levels (1−10 µmol L^{-1}). This interactive effect of CO_2 and phosphate may be due to their effects on Chl *a*.

311 The level of 2.8 μmol CO_2 ~~LC~~ induced more synthesis of Chl *a* at higher phosphate levels
312 (1−10 μmol L^{-1}). This induction of lower CO_2 ~~LC~~ on photosynthetic pigment is also reported
313 in green algae (Gao *et al.*, 2016). More energy is required under ~~LC~~ lower CO_2 to address the
314 more severe CO_2 limitation and thus more Chl *a* are synthesized to capture more light energy,
315 particularly when phosphate was replete. Although P is not an integral component for
316 chlorophyll, it plays an important role in cell energetics through high-energy phosphate bonds,
317 i.e. ATP, which could support chlorophyll synthesis. The stimulating effect of P enrichment on
318 photosynthetic pigment is also found in green alga *Dunaliella tertiolecta* (Geider *et al.*, 1998)
319 and brown alga *Sargassum muticum* (Xu *et al.*, 2017). The increased photosynthetic pigment
320 in *S. costatum* could partially explain the increased rETR and photosynthetic rate under the
321 higher P conditions.

322 *4.6. Ratio of respiration to photosynthesis*

323 The ratio of respiration to photosynthesis in algae indicates carbon balance in cells and
324 carbon flux in marine ecosystems as well (Zou & Gao, 2013).The level of 2.8 μmol CO_2 ~~LC~~
325 increased this ratio in *S. costatum* grown at the lower P conditions but did not affect it under
326 the higher P conditions, indicating that P enrichment can offset the carbon loss caused by
327 carbon limitation. To cope with CO_2 limitation, cells might have to obtain energy from dark
328 respiration under lower P conditions as it seems infeasible to acquire energy from the low
329 ~~r~~ETR, which led to the increased dark respiration. However, 2.8 μmol CO_2 ~~LC~~ induced higher
330 ~~r~~ETR under P replete conditions and energy used for inorganic carbon (CO_2 and HCO_3^-)
331 acquisition could be from the increased ~~r~~ETR. Therefore, additional dark respiration was not
332 triggered, avoiding carbon loss. Most studies regarding the effect of CO_2 on ratio of

respiration to photosynthesis focus on higher plants (Gifford, 1995; Ziska & Bunce, 1998; Cheng *et al.*, 2010; Smith & Dukes, 2013), little is known on phytoplankton. Our study suggests that CO_2 limitation may lead to carbon loss in phytoplankton but P enrichment could alter this trend, regulating carbon balance in phytoplankton and thus their capacity in carbon sequestration.

4.3. Inorganic carbon acquisition under CO_2 limitation and phosphate enrichment

Decreased CO_2 can usually induce higher inorganic carbon affinity in algae (Raven *et al.*, 2012; Wu *et al.*, 2012; Raven *et al.*, 2017; Xu *et al.*, 2017). In the present study, the lower CO_2 did increase inorganic carbon affinity when P level was higher than 0.25 μmol L^{-1} but did not affect it when P was 0.05 μmol L^{-1}, indicating the important role of P in regulating cells' CCMs in response to environmental CO_2 changes. The level of 2.8 μmol CO_2 ~~LC~~ induced larger CA activity when P was above 0.25 μmol L^{-1} but did not increase it at 0.05 μmol L^{-1} of P, which could explain the interactive effect of P and CO_2 on inorganic carbon affinity as CA can accelerate the equilibrium between HCO_3^- and CO_2 and increase inorganic carbon affinity. Regardless of CO_2, P enrichment alone increased CA activity and inorganic carbon affinity. P enrichment may stimulate the synthesis of CA by supplying required ATP. In addition, P enrichment increased the redox activity of plasma membrane in this study. It has been proposed that redox activity of plasma membrane could induce extracellular CA activity via protonation extrusion of its active center (Nimer *et al.*, 1998). Our result that the pattern of CA is exactly the same as that of redox activity of plasma membrane shows a compelling correlation between CA and redox activity of plasma membrane. The stimulating effect of P on redox activity of plasma membrane may be due to its effect on ~~r~~ETR. The increased ~~r~~ETR

could generate excess reducing equivalents, particularly under CO_2 limiting conditions. These excess reducing equivalents would be transported from the chloroplast into the cytosol (Heber, 1974), supporting the redox chain in the plasma membrane (Rubinstein & Luster, 1993; Nimer *et al.*, 1999) and triggering CA activity.

4.4. Direct HCO_3^- utilization due to phosphate enrichment

A pH compensation point over 9.2 has been considered a sign of direct HCO_3^- use for algae (Axelsson & Uusitalo, 1988) as the CO_2 concentration is nearly zero at pH above 9.2. This criterion has been justified based on ~~the~~ experiments for both micro and macro-algae. For instance, the marine diatom *Phaeodactylum tricornutum*, with a strong capacity for direct HCO_3^- utilization, has a higher pH compensation point of 10.3 (Chen *et al.*, 2006). In contrast, the red macroalgae, *Lomentaria articulata* and *Phycodrys rubens* that cannot utilize HCO_3^- directly, and whose photosynthesis only depends on CO_2 diffusion, have pH compensation points of less than 9.2 (Maberly, 1990). In terms of *S. costatum*, it has been reported to have a pH compensation point of 9.12, indicating a very weak capacity in direct HCO_3^- utilization (Chen & Gao, 2004). Our study demonstrates that the pH compensation point of *S. costatum* varies with the availability of P. It is lower than 9.2 under P limiting conditions but higher than 9.2 under P replete conditions, suggesting that the capacity of direct HCO_3^- utilization is regulated by P availability. Contrary to CO_2 passive diffusion, the direct use of HCO_3^- depends on positive transport that requires energy (Hopkinson & Morel, 2011). P enrichment increased ~~r~~ETR in the present study and the ATP produced during the process of electron transport could be used to support HCO_3^- positive transport. In addition, the increased respiration at higher P levels can also generate ATP to help HCO_3^- positive transport. Our

study indicates that P enrichment could trigger HCO_3^- direct utilization and hence increase inorganic acquisition capacity of *S. costatum* to cope with CO_2 limitation.

4.5. CCMs and red tides

In~~With~~ the development of red tides, the pH in seawater can~~ould~~ be very high along with extremely low CO_2 availability due to intensive photosynthesis (Hansen, 2002; Hinga, 2002). For instance, pH level in the surface waters of the eutrophic Mariager Fjord, Denmark, is often above 9 during dinoflagellate blooms (Hansen, 2002). Diatoms are the casautive species for red tides and *S. costatum* could outcompete other bloom algae (dinoflagellates *Prorocentrum minimum* and *Alexandrium tamarense*) under nutrient replete conditions (Hu *et al.*, 2011). However, the potential mechanisms are poorly understood. Our study demonstrates *S. costatum* has multiple CCMs to cope with CO_2 limitation and the operation of CCMs is regulated by P availability. The CCMs of *S. costatum* are hampered under P limiting conditions and only function when P is replete. This finding may explain why ~~Therefore, P enrichment would be critical for *S. costatum* to~~ diatoms could overcome carbon limitation ~~during algal bloom and to~~and dominate red tides when P is replete and as well as the shift from diatoms to dinoflagellates when P is limiting (Mackey et al., 2012).

5. Conclusions

The present study investigated the role of P in regulating inorganic carbon acquisition and CO_2 concentrating mechanisms in diatoms for the first time. The intensive photosynthesis and quick growth during algal blooms usually result in noticeable increase of pH and decrease of CO_2. Our study demonstrates that P enrichment could induce activity of extracellular carbonic anhydrase and direct utilization of HCO_3^- in *S. costatum* to help overcome ~~the~~ CO_2 limitation,

as well as increasing photosynthetic pigment content and rETR to provide required energy. This study provides important insight into the connection of phosphorus and carbon acquisition in diatoms and the mechanisms that help *S. costatum* dominates algal blooms.

Author contribution

JX and GG designed the experiments, and GG, JY, JF and XZ carried them out. GG prepared the manuscript with contributions from all co-authors.

Acknowledgements

This work was supported by National Natural Science Foundation of China (No. 41376156&40976078), Natural Science Fund of Guangdong Province (No. S2012010009853), the China Postdoctoral Science Foundation (2018T110463&2017M620270), Jiangsu Planned Projects for Postdoctoral Research Funds (1701003A), Science Foundation of Huaihai Institute of Technology (Z2016007), and Foundation for High-level Talents in Higher Education of Guangdong.

References

Alderkamp AC, Kulk G, Buma AG, Visser RJ, Van Dijken GL, Mills MM, Arrigo KR. 2012. The effect of iron limitation on the photophysiology of *Phaeocystis antarctica* (Prymnesiophyceae) and *Fragilariopsis cylindrus* (Bacillariophyceae) under dynamic irradiance. *Journal of Phycology* **48**: 45-59.

Anderson DM, Burkholder JM, Cochlan WP, Glibert PM, Gobler CJ, Heil CA, Kudela R, Parsons ML, Rensel JE, Townsend DW. 2008. Harmful algal blooms and eutrophication: Examining linkages from selected coastal regions of the United States. *Harmful Algae* **8**: 39-53.

带格式的：字体：加粗，检查拼写和语法

带格式的：缩进：左侧： 0 厘米，悬挂缩进： 3 字符

带格式的：字体：加粗，检查拼写和语法

421 **Axelsson L, Uusitalo J. 1988.** Carbon acquisition strategies for marine macroalgae. *Marine*
422 *Biology* **97**: 295-300.
423 **Barton AD, Irwin AJ, Finkel ZV, Stock CA. 2016.** Anthropogenic climate change drives
424 shift and shuffle in North Atlantic phytoplankton communities. *Proceedings of the*
425 *National Academy of Sciences, USA* **113**: 2964-2969.
426 **Beamud SG, Baffico GD, Reid B, Torres R, Gonzalez-Polo M, Pedrozo F, Diaz M. 2016.**
427 Photosynthetic performance associated with phosphorus availability in mats of
428 *Didymosphenia geminata* (Bacillariophyceae) from Patagonia (Argentina and Chile).
429 *Phycologia* **55**: 118-125.
430 **Beardall J, Roberts S, Raven JA. 2005.** Regulation of inorganic carbon acquisition by
431 phosphorus limitation in the green alga *Chlorella emersonii*. *Canadian Journal of*
432 *Botany* **83**: 859-864.
433 **Berg GM, Glibert PM, Lomas MW, Burford MA. 1997.** Organic nitrogen uptake and
434 growth by the chrysophyte *Aureococcus anophagefferens* during a brown tide event.
435 *Marine Biology* **129**: 377-387.
436 **Brembu T, Mühlroth A, Alipanah L, Bones AM. 2017.** The effects of phosphorus limitation
437 on carbon metabolism in diatoms. *Philosophical Transactions of the Royal Society B*
438 *Biological Sciences* **372**: 20160406.
439 **Bruland KW, Rue EL, Smith GJ. 2001.** Iron and macronutrients in california coastal
440 upwelling regimes: implications for diatom blooms. *Limnology and Oceanography* **46**:
441 1661-1674.
442 **Caemmerer SV, Farquhar GD. 1981.** Some relationships between the biochemistry of

photosynthesis and the gas exchange of leaves. *Planta* 153: 376-387.

Chen X, Gao K. 2004. Photosynthetic utilisation of inorganic carbon and its regulation in the marine diatom *Skeletonema costatum*. *Functional Plant Biology* **31**: 1027-1033.

Chen X, Qiu CE, Shao JZ. 2006. Evidence for K^+-dependent HCO_3^- utilization in the marine diatom *Phaeodactylum tricornutum*. *Plant Physiology* **141**: 731-736.

Cheng W, Sims DA, Luo Y, Coleman JS, Johnson DW. 2010. Photosynthesis, respiration, and net primary production of sunflower stands in ambient and elevated atmospheric CO_2 concentrations: an invariant NPP:GPP ratio? *Global Change Biology* **6**: 931-941.

Davies AG, Sleep JA. 1989. The photosynthetic response of nutrient-depleted dilute cultures of *Skeletonema costatum* to pulses of ammonium and nitrate; the importance of phosphate. *Journal of Plankton Research* **11**: 141-164.

Dickson AG. 1990. Standard potential of the reaction: AgCl(s) + 12H2(g) = Ag(s) + HCl(aq), and the standard acidity constant of the ion HSO_4^- in synthetic sea water from 273.15 to 318.15 K. *Journal of Chemical Thermodynamics* **22**: 113-127.

Dimier C, Brunet C, Geider R, Raven J. 2009. Growth and photoregulation dynamics of the picoeukaryote *Pelagomonas calceolata* in fluctuating light. *Limnology and Oceanography* **54**: 823-836.

Ennos AR. 2007. Statistical and Data Handling Skills in Biology. Pearson Education, p.96.

Falkowski P. 2012. Ocean Science: The power of plankton. *Nature* **483**: 17-20.

Field CB, Behrenfeld MJ, Randerson JT, Falkowski P. 1998. Primary production of the biosphere: integrating terrestrial and oceanic components. *Science* **281**: 237-240.

Gao G, Clare AS, Rose C, Caldwell GS. 2018a. *Ulva rigida* in the future ocean: potential for carbon capture, bioremediation, and biomethane production. *Global Change*

带格式的：字体：加粗

带格式的：正文，缩进：左侧： 0 厘米，悬挂缩进：3 字符，首行缩进： -3 字符

带格式的：字体：倾斜

带格式的：字体：加粗

Biology Bioenergy **10:** 39-51.

Gao G, Gao K, Giordano M. 2009. Responses to solar UV radiation of the diatom *Skeletonema costatum* (Bacillariophyceae) grown at different Zn^{2+} concentrations *Journal of Phycology* **45**: 119-129.

Gao G, Liu Y, Li X, Feng Z, Xu J. 2016. An ocean acidification acclimatised green tide alga Is robust to changes of seawater carbon chemistry but vulnerable to light stress. *PloS One* **11**: e0169040.

Gao G, Xia J, Yu J, Zeng X. 2018b. Physiological response of a red tide alga (*Skeletonema costatum*) to nitrate enrichment, with special reference to inorganic carbon acquisition. *Marine Environmental Research*, **133:** 15-23.

Geider RJ, Macintyre HL, Graziano LM, McKay RML. 1998. Responses of the photosynthetic apparatus of *Dunaliella tertiolecta* (Chlorophyceae) to nitrogen and phosphorus limitation. *European Journal of Phycology* **33**: 315-332.

Gifford RM. 1995. Whole plant respiration and photosynthesis of wheat under increased CO_2 concentration and temperature: long-term vs. short-term distinctions for modelling. *Global Change Biology* **1**: 385–396.

Hansen PJ. 2002. Effect of high pH on the growth and survival of marine phytoplankton: implications for species succession. *Aquatic Microbial Ecology* **28**: 279-288.

Heber U. 1974. Metabolite exchange between chloroplasts and cytoplasm. *Annual Review of Plant Physiology* **25**: 393-421.

Hinga KR. 2002. Effects of pH on coastal marine phytoplankton. *Marine Ecology Progress Series* **238**: 281-300.

Hopkinson BM, Dupont CL, Matsuda Y. 2016. The physiology and genetics of CO_2 concentrating mechanisms in model diatoms. *Current Opinion in Plant Biology* **31**: 51-57.

Hopkinson BM, Morel FMM. 2011. Efficiency of the CO_2-concentrating mechanism of diatoms. *Proceedings of the National Academy of Sciences, USA* **108**: 3830-3837.

Hu H, Zhang J, Chen W. 2011. Competition of bloom-forming marine phytoplankton at low nutrient concentrations. *Journal of Environmental Sciences* **23**: 656-663.

Hu H, Zhou Q. 2010. Regulation of inorganic carbon acquisition by nitrogen and phosphorus levels in the *Nannochloropsis* sp. *World Journal of Microbiology & Biotechnology* **26**: 957-961.

Jeong HJ, An SL, Franks PJS, Lee KH, Ji HK, Kang NS, Lee MJ, Jang SH, Lee SY, Yoon EY. 2015. A hierarchy of conceptual models of red-tide generation: Nutrition, behavior, and biological interactions. *Harmful Algae* **47**: 97-115.

Jiang X, Han Q, Gao X, Gao G. 2016. Conditions optimising on the yield of biomass, total lipid, and valuable fatty acids in two strains of *Skeletonema menzelii*. *Food Chemistry* **194**: 723-732.

Lefebvre S, Mouget JL, Loret P, Rosa P, Tremblin G. 2007. Comparison between fluorimetry and oximetry techniques to measure photosynthesis in the diatom *Skeletonema costatum* cultivated under simulated seasonal conditions. *Journal of Photochemistry and Photobiology B: Biology* **86**: 131-139.

Li G, Gao K, Yuan D, Zheng Y, Yang G. 2011. Relationship of photosynthetic carbon fixation with environmental changes in the Jiulong River estuary of the South China

带格式的: 字体: 加粗

带格式的: Default, 缩进: 左侧: 0 厘米, 悬挂缩进: 3 字符, 首行缩进: -3 字符

带格式的: 字体: 倾斜

带格式的: 字体: 加粗

Sea, with special reference to the effects of solar UV radiation. *Marine Pollution Bulletin* **62**: 1852-1858.

Lin S, Litaker RW, Sunda WG. 2016. Phosphorus physiological ecology and molecular mechanisms in marine phytoplankton. *Journal of Phycology* **52**: 10.

Liu Y, Song X, Cao X, Yu Z. 2012. Responses of photosynthetic characters of *Skeletonema costatum* to different nutrient conditions. *Journal of Plankton Research* **35**: 165-176.

Maberly SC. 1990. Exogenous sources of inorganic carbon for photosynthesis by marine macroalgae. *Journal of Phycology* **26**: 439-449.

Mackey KRM, Mioni CE, Ryan JP, Paytan A. 2012. Phosphorus cycling in the red tide incubator region of Monterey Bay in response to upwelling. Frontiers in Microbiology, **3**: 33.

Mccall SJ, Hale MS, Smith JT, Read DS, Bowes MJ. 2017. Impacts of phosphorus concentration and light intensity on river periphyton biomass and community structure. *Hydrobiologia* **792**: 315-330.

Moore CM, Mills MM, Arrigo KR, Bermanfrank I, Bopp L, Boyd PW, Galbraith ED, Geider RJ, Guieu C, Jaccard SL. 2013. Processes and patterns of oceanic nutrient limitation. *Nature Geoscience* **6**: 701-710.

Müller S, Mitrovic SM. 2015. Phytoplankton co-limitation by nitrogen and phosphorus in a shallow reservoir: progressing from the phosphorus limitation paradigm. *Hydrobiologia* **744**: 255-269.

Nelson DM, Tréguer P, Brzezinski MA, Leynaert A, Quéguiner B. 1995. Production and dissolution of biogenic silica in the ocean: Revised global estimates, comparison with

带格式的：字体：加粗

带格式的：字体：加粗

regional data and relationship to biogenic sedimentation. *Global Biogeochemical Cycles* **9**: 359-372.

Nimer NA, Ling MX, Brownlee C, Merrett MJ. 1999. Inorganic carbon limitation, exofacial carbonic anhydrase activity, and plasma membrane redox activity in marine phytoplankton species. *Journal of Phycology* **35**: 1200-1205.

Nimer NA, Warren M, Merrett MJ. 1998. The regulation of photosynthetic rate and activation of extracellular carbonic anhydrase under CO_2-limiting conditions in the marine diatom *Skeletonema costatum*. *Plant Cell and Environment* **21**: 805–812.

Pierrot D, Lewis E, Wallace DWR. 2006. MS Excel program developed for CO_2 system calculations. *ORNL/CDIAC-105a. Carbon Dioxide Information Analysis Center, Oak Ridge National Laboratory, US Department of Energy, Oak Ridge, Tennessee*.

Raven JA, Beardall J, Sánchez-Baracaldo P. 2017. The possible evolution, and future, of CO2-concentrating mechanisms. *Journal of Experimental Botany*.

Raven JA, Giordano M, Beardall J, Maberly SC. 2012. Algal evolution in relation to atmospheric CO2: carboxylases, carbon-concentrating mechanisms and carbon oxidation cycles. *Phil. Trans. R. Soc. B* **367**: 493-507.

Reed ML, Pinckney JL, Keppler CJ, Brock LM, Hogan SB, Greenfield DI. 2016. The influence of nitrogen and phosphorus on phytoplankton growth and assemblage composition in four coastal, southeastern USA systems. *Estuarine Coastal & Shelf Science* **177**: 71-82.

Rost B, Riebesell U, Burkhardt S, Sültemeyer D. 2003. Carbon acquisition of bloom-forming marine phytoplankton. *Limnology and Oceanography* **48**: 55-67.

554 **Roy RN, Roy LN, Vogel KM, Porter-Moore C, Pearson T, Good CE, Millero FJ,**
555 **Campbell DM. 1993.** The dissociation constants of carbonic acid in seawater at
556 salinities 5 to 45 and temperatures 0 to 45^{o}C. *Marine Chemistry* **44**: 249-267.
557 **Rubinstein B, Luster DG. 1993.** Plasma membrane redox activity: components and role in
558 plant processes. *Annual Review of Plant Biology* **44**: 131-155.
559 **Smetacek V, Zingone A. 2013.** Green and golden seaweed tides on the rise. *Nature* **504**:
560 84-88.
561 **Smith NG, Dukes JS. 2013.** Plant respiration and photosynthesis in global-scale models:
562 incorporating acclimation to temperature and CO_2. *Global Change Biology* **19**: 45-63.
563 **Wang J. 2002.** Phytoplankton communities in three distinct ecotypes of the Changjiang
564 estuary. *Journal of Ocean University of China* **32**: 422-428.
565 **Wu X, Gao G, Giordano M, Gao K. 2012.** Growth and photosynthesis of a diatom grown
566 under elevated CO_2 in the presence of solar UV radiation. *Fundamental and Applied*
567 *Limnology* **180**: 279-290.
568 **Xu Z, Gao G, Xu J, Wu H. 2017.** Physiological response of a golden tide alga (*Sargassum*
569 *muticum*) to the interaction of ocean acidification and phosphorus enrichment.
570 *Biogeosciences* **14**: 671-681.
571 **Young JN, Morel FMM. 2015.** Biological oceanography: The CO_2 switch in diatoms. *Nature*
572 *Climate Change* **5**: 722-723.
573 **Ziska LH, Bunce JA. 1998.** The influence of increasing growth temperature and CO_2
574 concentration on the ratio of respiration to photosynthesis in soybean seedlings.
575 *Global Change Biology* **4**: 637-643.

Zou D, Gao K. 2013. Thermal acclimation of respiration and photosynthesis in the marine macroalga *Gracilaria lemaneiformis* (Gracilariales, Rhodophyta). *Journal of Phycology* **49**: 61–68.

581 Table 1 Two-way analysis of variance for the effects of CO_2 and phosphate on net
582 photosynthetic rate, dark respiration rate and ratio of respiration to photosynthesis of *S.*
583 *costatum*. CO_2*phosphate means the interactive effect of CO_2 and phosphate, df means degree
584 of freedom, F means the value of F statistic, and Sig. means p-value.

585

Source	Net photosynthetic rate			Dark respiration rate			Ratio of respiration to photosynthesis		
	df	F	Sig.	df	F	Sig.	df	F	Sig.
CO_2	1	11.286	0.003	1	1.262	0.275	1	32.443	<0.001
Phosphate	4	157.925	<0.001	4	169.050	<0.001	4	7.081	0.001
CO_2*phosphate	4	3.662	0.021	4	3.226	0.034	4	8.299	<0.001
Error	20			20			20		

586 Table 2 Two-way analysis of variance for the effects of CO_2 and phosphate on relative
587 electron transport rate (rETR), Chl *a*, and CO_2 level required to give half of DIC-saturated
588 maximum rate of photosynthetic O_2 evolution ($K_{0.5}$) of *S. costatum*. CO_2*phosphate means the
589 interactive effect of CO_2 and phosphate, df means degree of freedom, F means the value of F
590 statistic, and Sig. means p-value.

591

Source	rETR			Chl *a*			$K_{0.5}$		
	df	F	Sig.	df	F	Sig.	df	F	Sig.
CO_2	1	28.717	<0.001	1	32.963	<0.001	1	96.182	<0.001
Phosphate	4	127.860	<0.001	4	92.045	<0.001	4	40.497	<0.001
CO_2*phosphate	4	3.296	0.031	4	3.871	0.017	4	3.821	0.018
Error	20			20			20		

592 Table 3 Two-way analysis of variance for the effects of CO_2 and phosphate on CA_{ext} activity,
593 redox activity of plasma membrane and pH compensation point of *S. costatum*.
594 CO_2*phosphate means the interactive effect of CO_2 and phosphate, df means degree of
595 freedom, F means the value of F statistic, and Sig. means p-value.

596

Source	CA_{ext} activity			redox activity of plasma membrane			pH compensation point		
	df	F	Sig.	df	F	Sig.	df	F	Sig.
CO_2	1	569.585	<0.001	1	937.963	<0.001	1	0.056	0.816
Phosphate	4	176.392	<0.001	4	276.362	<0.001	4	226.196	<0.001
CO_2*phosphate	4	87.380	<0.001	4	137.050	<0.001	4	0.040	0.997
Error	20			20			20		

597 Table 4 Repeated measures analysis of variance for the effects of CO_2 and phosphate on pH
598 change during 10 hours of incubation. Time*CO_2 means the interactive effect of incubation
599 time and CO_2, Time*phosphate means the interactive effect of incubation time and phosphate,
600 Time*CO_2*phosphate means the interactive effect of incubation time, CO_2 and phosphate,
601 df means degree of freedom, F means the value of F statistic, and Sig. means p-value.

Source	Type III Sum of Squares	df	Mean Square	F	Sig.
Time	40.766	10	4.077	8737.941	<0.001
Time*CO_2	0.003	10	<0.001	0.569	0.838
Time*phosphate	0.886	40	0.022	47.496	<0.001
Time*CO_2*phosphate	0.002	40	<0.001	0.112	1.000
Error	0.093	200	<0.001		

602 **Figure legends**

603 **Fig. 1.** Net photosynthetic rate (a) ~~and,~~ dark respiration rate (b) and ratio of respiration rate to
604 net photosynthetic rate (c) in *S. costatum* grown at various phosphate concentrations after
605 12.6~~ambient (AC)~~ and 2.8 µmol CO_2 ~~low CO_2 (LC)~~ treatments. The error bars indicate the
606 standard deviations (n = 3). ~~Different letters represent the significant difference ($P < 0.05$)~~
607 ~~among phosphate concentrations (capital for AC, lower case for LC). Horizontal lines~~
608 ~~represent significant difference ($P < 0.05$) between CO_2 treatments.~~
609 ~~**Fig. 2.** Ratio of respiration rate to net photosynthetic rate in *S. costatum* grown at various~~
610 ~~phosphate concentrations after ambient (AC) and low CO_2 (LC) treatments. The error bars~~
611 ~~indicate the standard deviations (n = 3). Different letters represent the significant difference (P~~
612 ~~< 0.05) among phosphate concentrations (capital for AC, lower case for LC). Horizontal lines~~
613 ~~represent significant difference ($P < 0.05$) between CO_2 treatments.~~
614 **Fig. ~~3~~2.** Relative electron transport rate (rETR) in *S. costatum* grown at various phosphate
615 concentrations after 12.6 and 2.8 µmol CO_2~~ambient (AC) and low CO_2 (LC)~~ treatments. The
616 error bars indicate the standard deviations (n = 3). ~~Different letters represent the significant~~
617 ~~difference ($P < 0.05$) among phosphate concentrations (Capital for AC lower case for LC).~~
618 ~~Horizontal lines represent significant difference ($P < 0.05$) between CO_2 treatments.~~
619 **Fig. 43.** Photosynthetic Chl *a* content in *S. costatum* grown at various phosphate
620 concentrations after 12.6 and 2.8 µmol CO_2~~ambient (AC) and low CO_2 (LC)~~ treatments. The
621 error bars indicate the standard deviations (n = 3). ~~Different letters represent the significant~~
622 ~~difference ($P < 0.05$) among phosphate concentrations (capital for AC, lower case for LC).~~
623 ~~Horizontal lines represent significant difference ($P < 0.05$) between CO_2 treatments.~~

Fig. ~~5~~4. Net photosynthetic rate as a function of DIC for *S. costatum* grown at various phosphate concentrations after 12.6 ~~ambient~~ (a) and~~–~~ 2.8 µmol CO_2~~low CO_2~~ (b) treatments. The error bars indicate the standard deviations (n = 3).

Fig. ~~6~~5. Half saturation constant ($K_{0.5}$) for CO_2 in *S. costatum* grown at at various phosphate concentrations after 12.6 and 2.8 µmol CO_2~~ambient (AC) and low CO_2 (LC)~~ treatments. The error bars indicate the standard deviations (n = 3). ~~Different letters represent the significant difference ($P < 0.05$) among phosphate concentrations (capital for AC, lower case for LC). Horizontal lines represent significant difference ($P < 0.05$) between CO_2 treatments.~~

Fig. ~~7~~6. CA_{ext} activity (a) and reduction rate of ferricyanide (b) in *S. costatum* grown at various phosphate concentrations after 12.6 and 2.8 µmol CO_2~~ambient (AC) and low CO_2 (LC)~~ treatments. The error bars indicate the standard deviations (n = 3). ~~Different letters represent the significant difference ($P < 0.05$) among phosphate concentrations (capital for AC, lower case for LC). Horizontal lines represent significant difference ($P < 0.05$) between CO_2 treatments.~~

Fig. ~~8~~7. Changes of pH in a closed system caused by photosynthesis of *S. costatum* grown at various phosphate concentrations after 12.6 and 2.8 µmol CO_2~~ambient (AC) and low CO_2 (LC)~~ treatments. The error bars indicate the standard deviations (n = 3).

带格式的: 字体: Times New Roman, 小四, 字体颜色: 文字 1

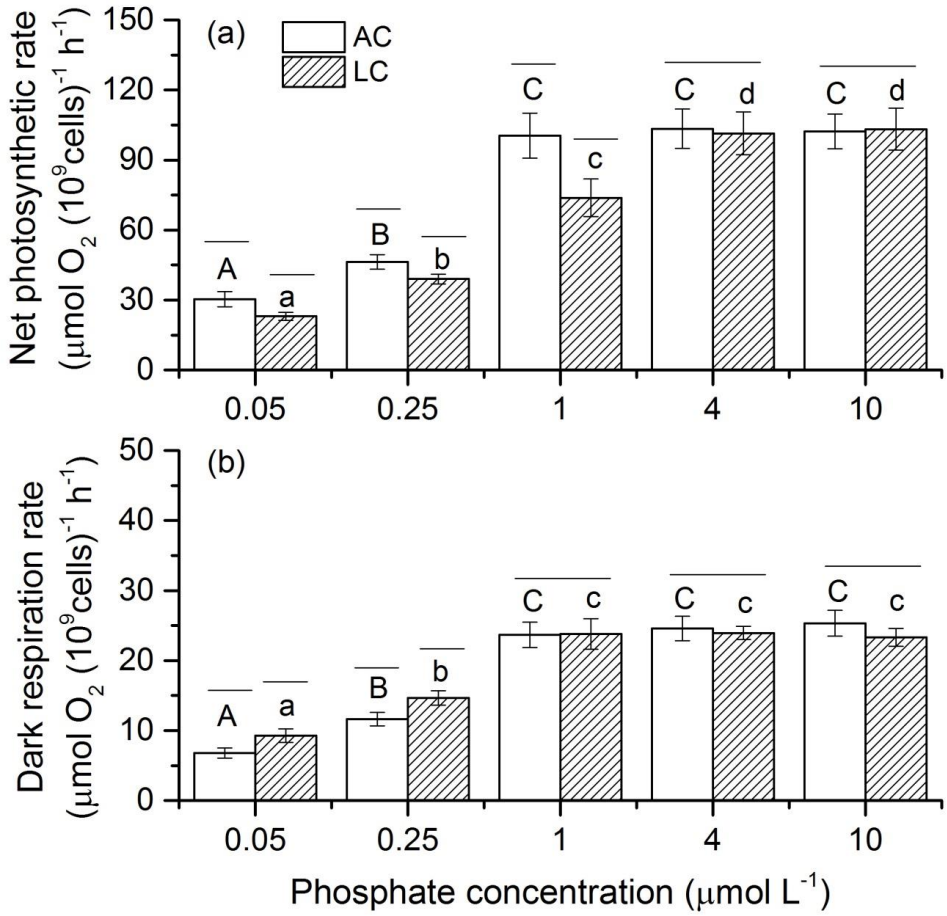

641

带格式的: 字体: Times New Roman, 小四, 字体颜色: 文字 1

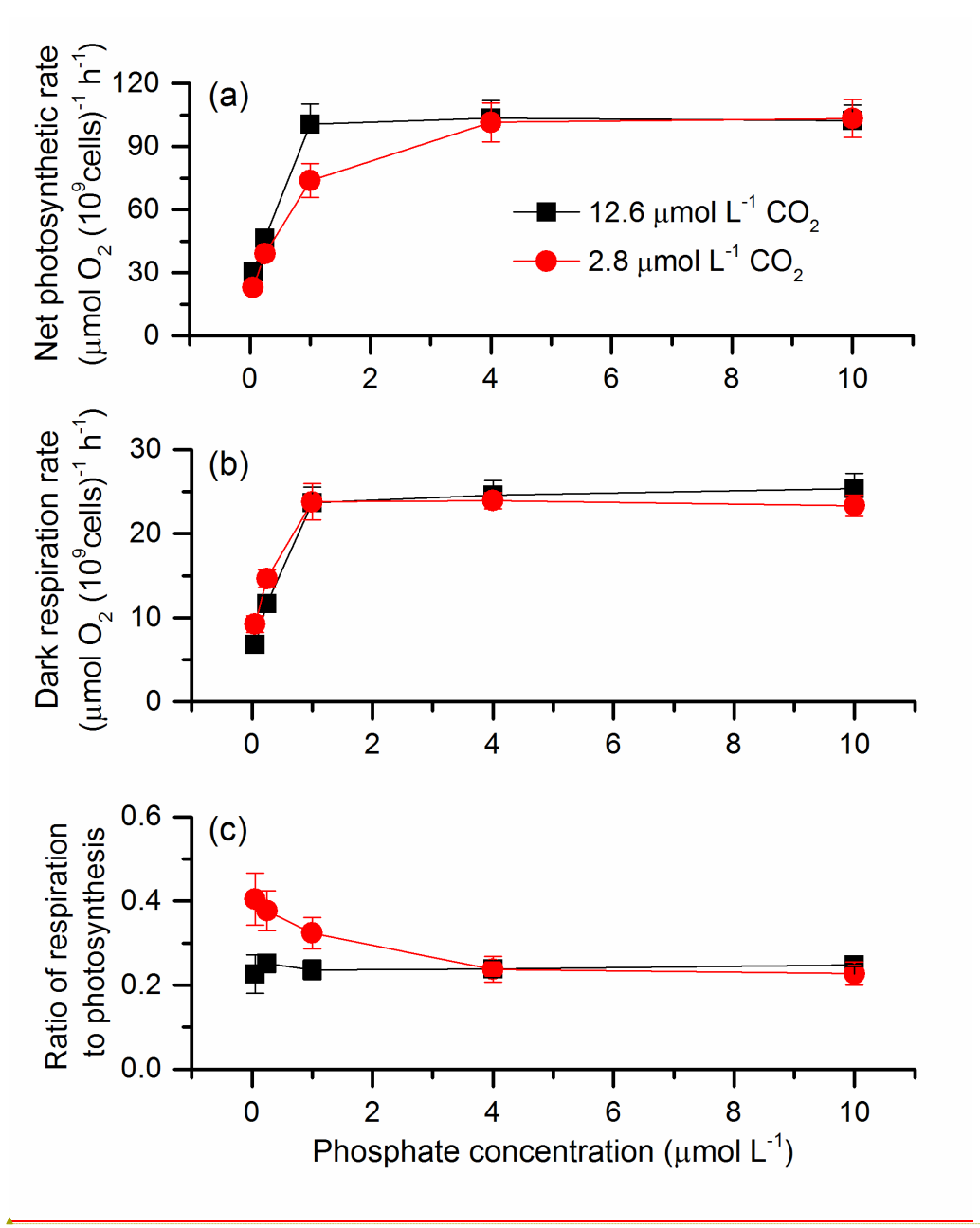

Fig. 1

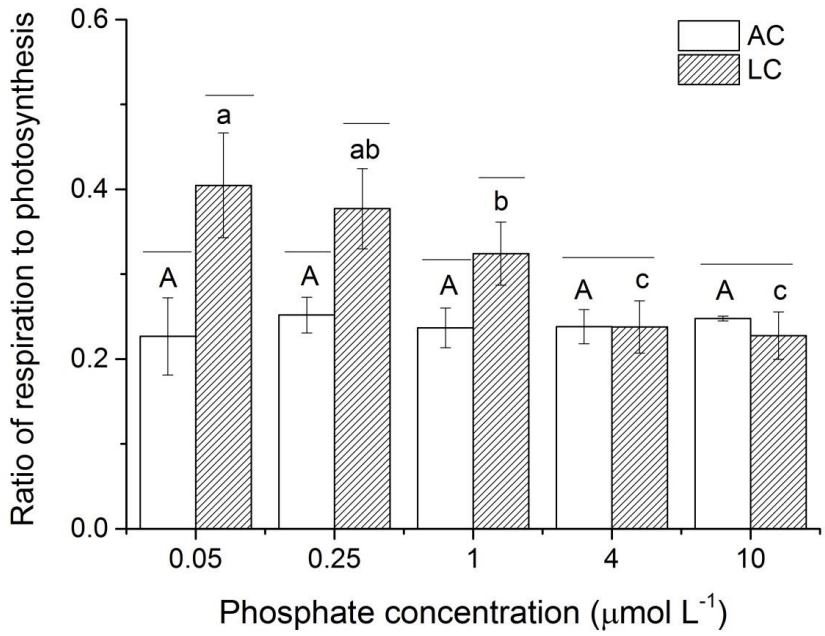

644

645 **~~Fig. 2~~**

带格式的：字体：Times New Roman，小四，加粗，字体颜色：文字 1

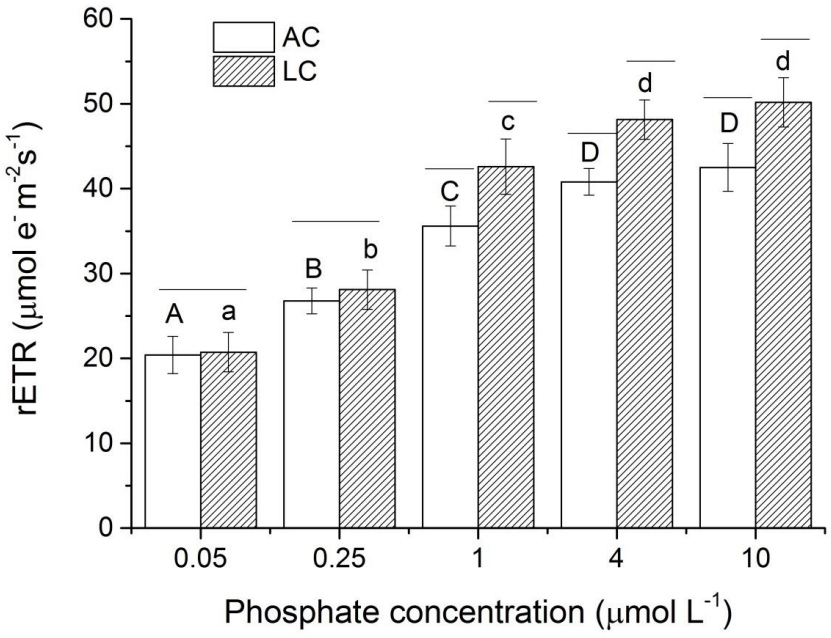
AC
LC
rETR (μmol e⁻ m⁻² s⁻¹)
60
50
40
30
20
10
0
A
a
B
b
C
c
D
d
D
d
0.05
0.25
1
4
10
Phosphate concentration (μmol L⁻¹)

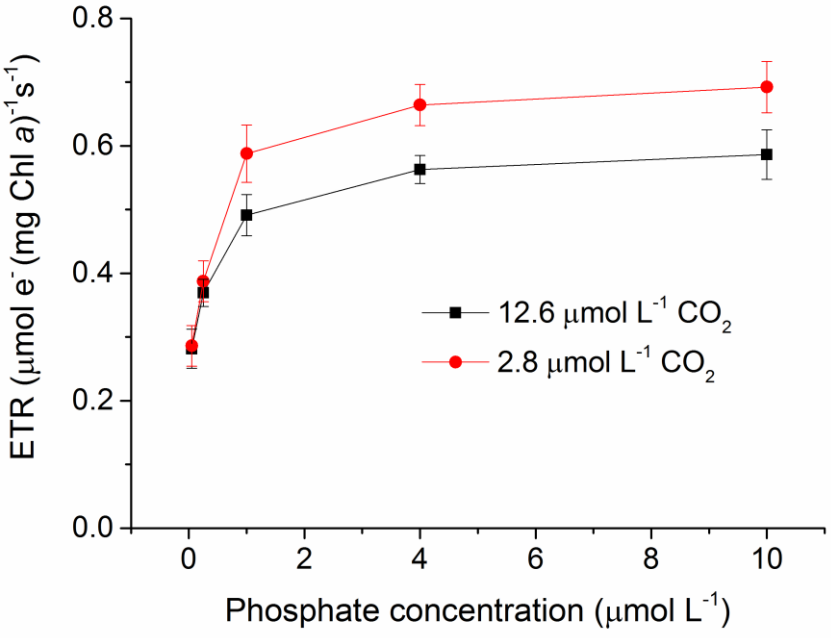
ETR (μmol e⁻ (mg Chl a)⁻¹ s⁻¹)
0.8
0.6
0.4
0.2
0.0
12.6 μmol L⁻¹ CO₂
2.8 μmol L⁻¹ CO₂
0
2
4
6
8
10
Phosphate concentration (μmol L⁻¹)

Fig. ~~3~~2

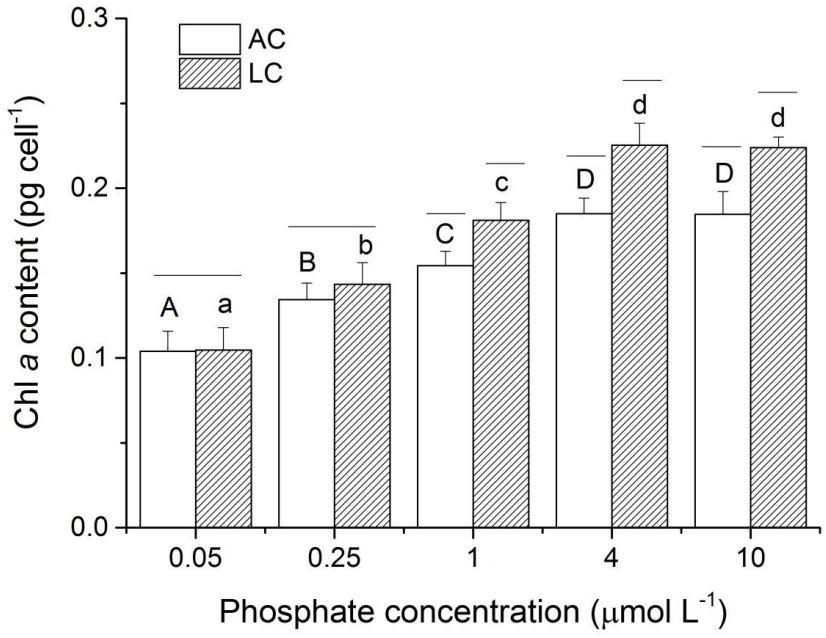
AC
LC
Chl a content (pg cell-1)
0.3
0.2
0.1
0.0
A
a
B
b
C
c
D
d
D
d
0.05
0.25
1
4
10
Phosphate concentration (μmol L-1)

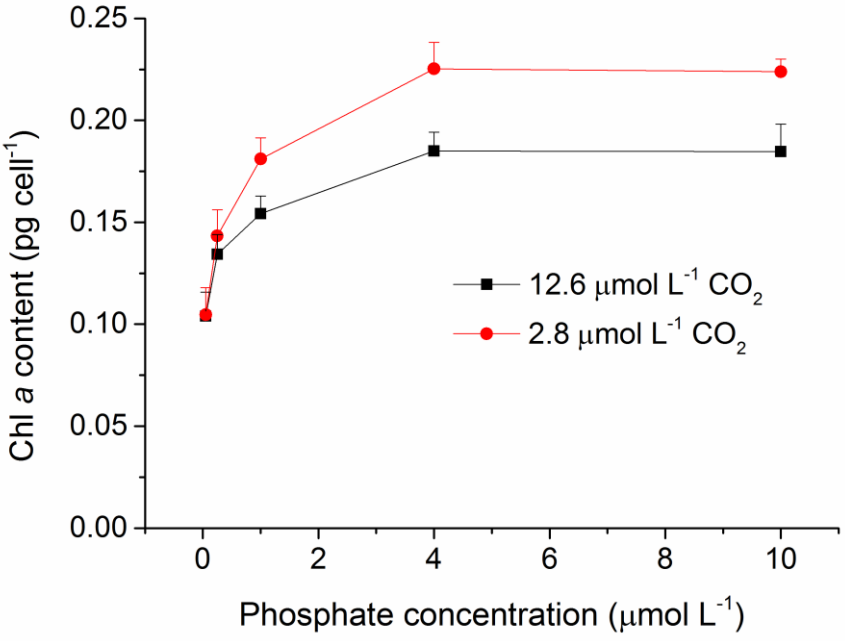
Chl a content (pg cell-1)
0.25
0.20
0.15
0.10
0.05
0.00
12.6 μmol L-1 CO2
2.8 μmol L-1 CO2
0
2
4
6
8
10
Phosphate concentration (μmol L-1)

Fig. 43

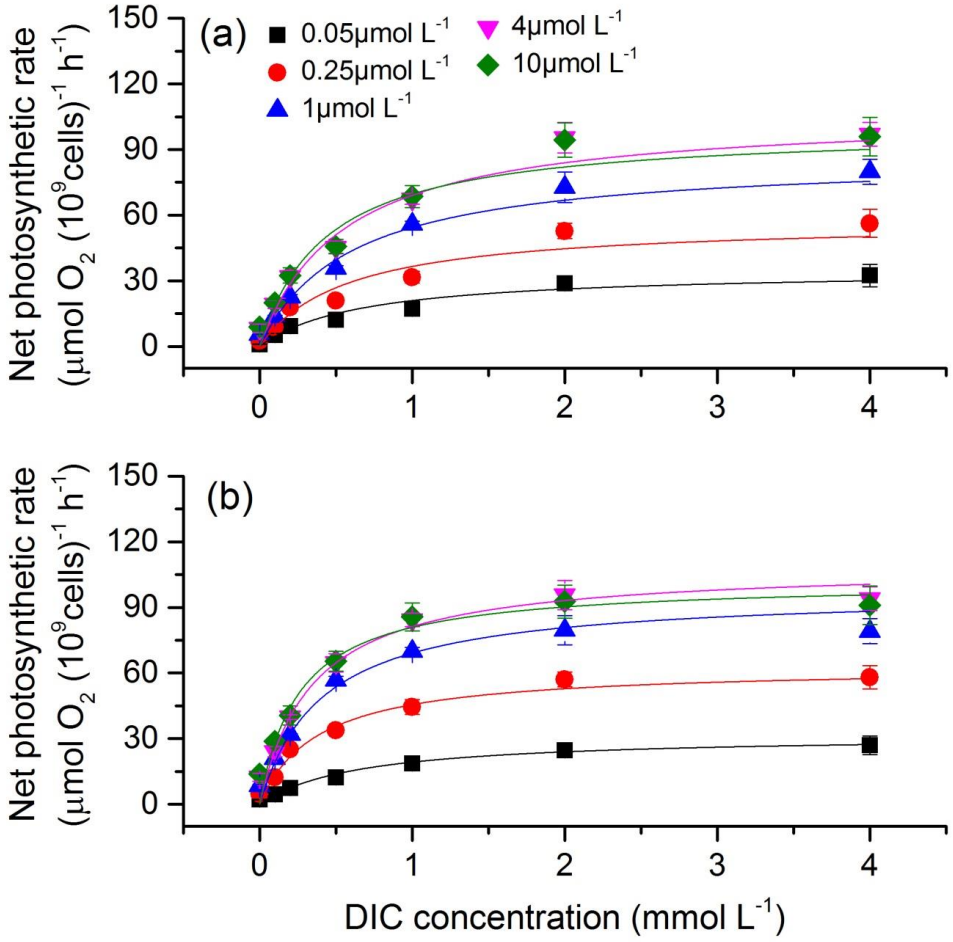

652

653 **Fig. ~~5~~4**

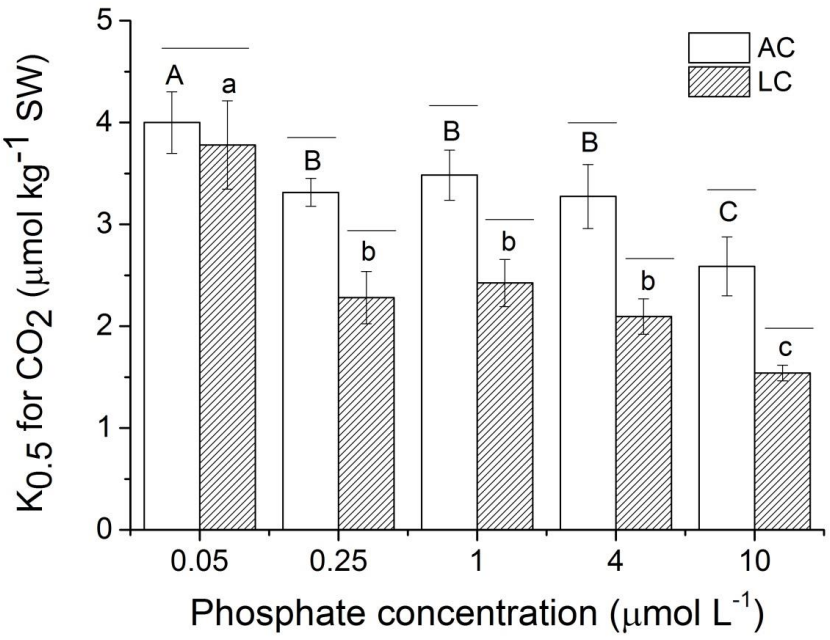
AC
LC
A
a
B
b
B
b
B
b
C
c
$K_{0.5}$ for CO_2 (μmol kg^{-1} SW)
0
1
2
3
4
5
0.05
0.25
1
4
10
Phosphate concentration (μmol L^{-1})

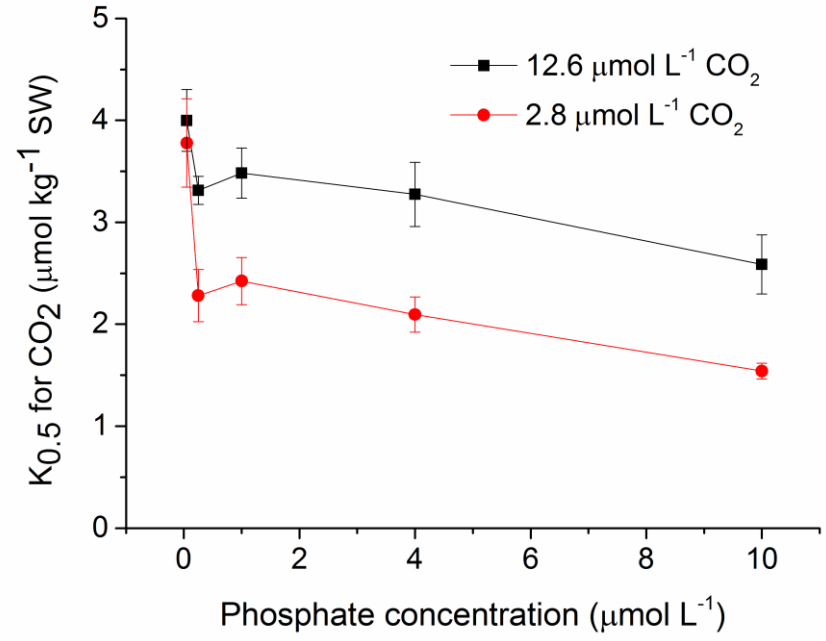
12.6 μmol L^{-1} CO_2
2.8 μmol L^{-1} CO_2
$K_{0.5}$ for CO_2 (μmol kg^{-1} SW)
0
1
2
3
4
5
0
2
4
6
8
10
Phosphate concentration (μmol L^{-1})

Fig. ~~6~~5

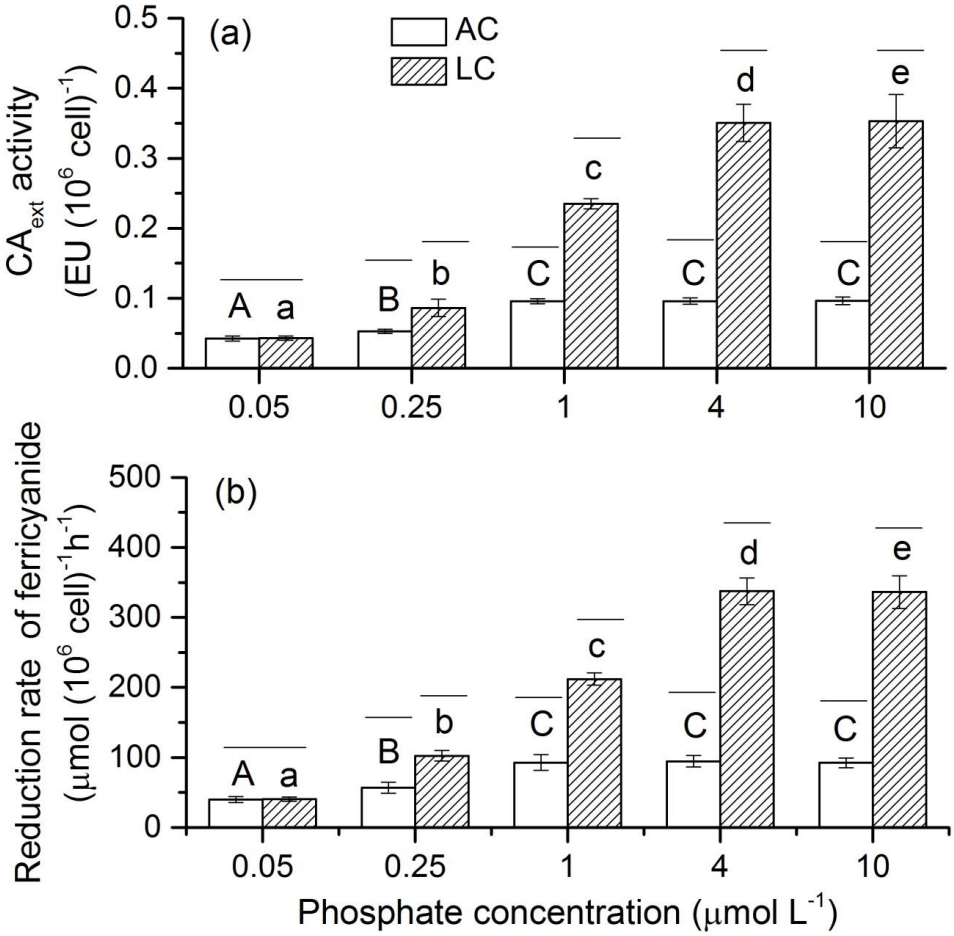

657

带格式的: 字体: Times New Roman, 小四, 加粗, 字体颜色: 文字 1

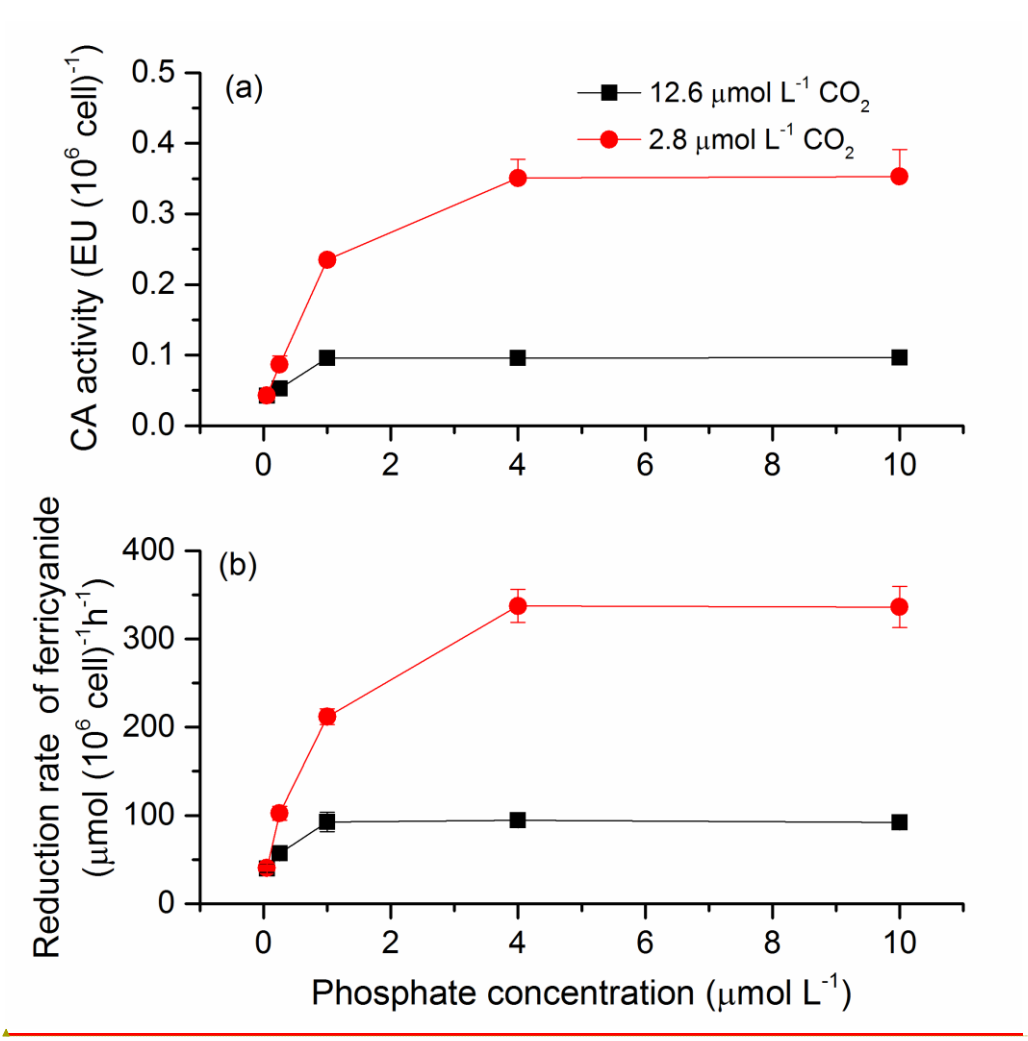

Fig. ~~7~~6

带格式的: 字体: Times New Roman, 小四, 加粗, 字体颜色: 文字 1

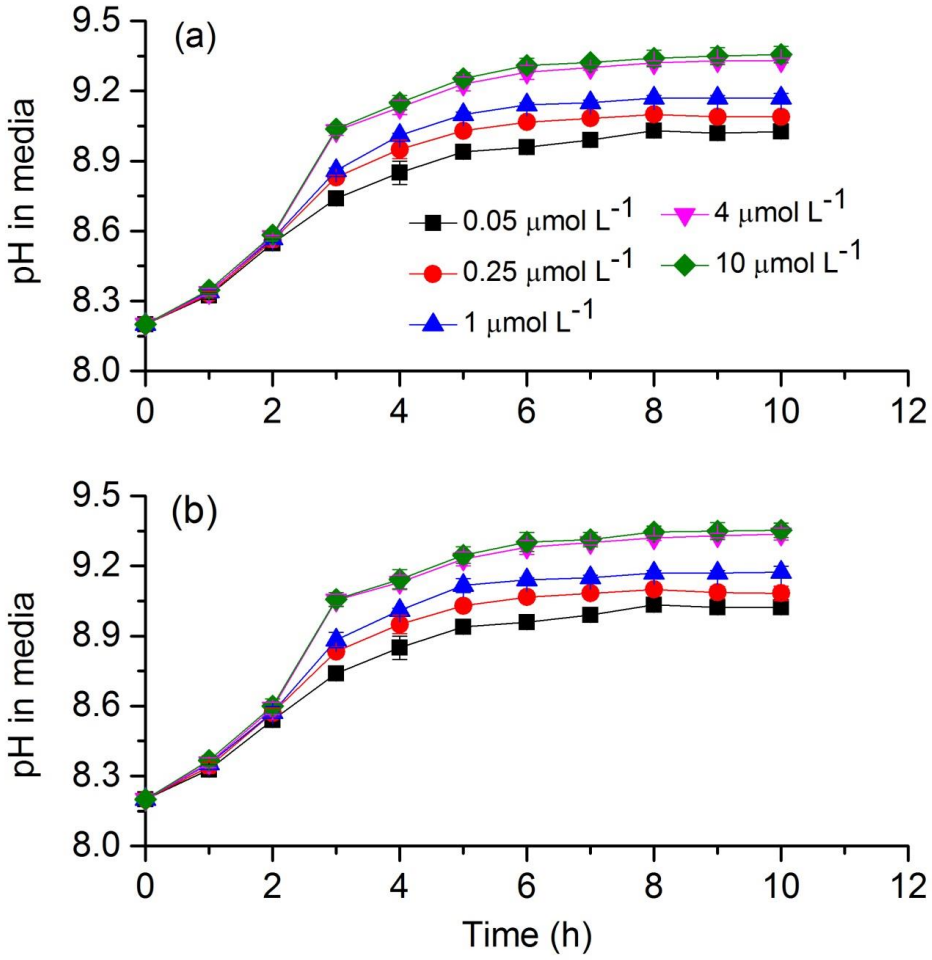
(a)
(b)
pH in media
Time (h)
0.05 μmol L-1
0.25 μmol L-1
1 μmol L-1
4 μmol L-1
10 μmol L-1
9.5
9.2
8.9
8.6
8.3
8.0
0
2
4
6
8
10
12

Fig. ~~8~~7